Food and Bioprocess Technology (2025) 18:8845–8860
https://doi.org/10.1007/s11947-025-03965-9

RESEARCH

Advancing 3D-Printed Seafood Analogues with *Tetraselmis chui* and *Tetraselmis chui* Water Extract

Catarina Moreira[1] · Carmen Molina-Montero[2] · Pedro Ferreira-Santos[3,4] · José A. Teixeira[1,5] · Cristina M. R. Rocha[1,5] · Javier Martínez-Monzó[2]

Received: 2 May 2025 / Accepted: 8 July 2025 / Published online: 22 July 2025
© The Author(s) 2025

Abstract

The urgent need for sustainable agrifood practices has driven the exploration of alternative protein sources. This study investigates the potential of *Tetraselmis chui* and its extract as ingredients in 3D-printed seafood analogues. The rheological, textural, and color properties of *Tetraselmis chui* and *Tetraselmis chui's* extract were compared with pea protein. The results demonstrated that *Tetraselmis chui* and *Tetraselmis chui's* extract combined with pea protein can be effectively used in 3D food printing, with *Tetraselmis chui* showing superior structural integrity and rheological properties to *Tetraselmis chui* extract. The incorporation of *Tetraselmis chui* and *Tetraselmis chui's* extract influenced the texture and color of the printed products, with *Tetraselmis chui* providing a more stable gel structure. This research highlights the potential of microalgae as a sustainable ingredient in developing plant-based seafood alternatives, contributing to the advancement of eco-friendly food production technologies.

Keywords Microalgae · 3D printing · Rheology · Texture · Color

Introduction

The urgent need for sustainable practices, especially in agrifood, is driven by climate change, diminishing land and water resources, increasing pollution, and declining biodiversity (Kazir & Livney, 2021). The growth in demand for animal-derived products outpaces global population growth (United Nations, 2019), making it impossible for animal-based agrifood production to meet this rising consumption. This unsustainable production leads to detrimental ecological and health impacts, as well as animal welfare concerns (The Good Food Institute, 2022). A significant part of addressing this issue involves replacing animal-based foods, particularly beef and fish, with sustainable, eco-friendly alternatives.

Recent research has focused significantly on the creation of plant-protein hydrogel-based foods as alternatives (Hadidi et al., 2022; Wen et al., 2023; Zhong et al., 2023). These hydrogels are commonly produced using plant proteins from sources such as rice, soy, and pea, among others. However, compared to animal-based protein gels with equivalent protein concentrations, gels derived from plant proteins that are induced by heat tend to be weaker (Ren et al., 2024). Recent research has proposed

Highlights
- *T. chui* shown to be a potential ingredient to replace pea protein
- Extrusion forces over 38 N were required to print the seafood analog
- *T. chui* water extract formulations did not show structural integrity after printing
- *T. chui* and *T. chui's* extract influenced both texture and color

✉ Javier Martínez-Monzó
xmartine@tal.upv.es

1 Centre of Biological Engineering, University of Minho, Campus de Gualtar, 4710-057 Braga, Portugal

2 I-FOOD, Instituto Universitario de Ingeniería de Alimentos-FoodUPV, Universitat Politècnica de València, Valencia, Spain

3 Department of Chemical Engineering, Faculty of Science, University of Vigo, As Lagoas, 32004 Ourense, Spain

4 Instituto de Agroecoloxía E Alimentación (IAA), University of Vigo (Campus Auga), As Lagoas, 32004 Ourense, Spain

5 LABBELS - Associate Laboratory, Guimarães, Braga, Portugal

various methods to improve their mechanical characteristics. Among these strategies, incorporating polysaccharides into protein-based gels has emerged as one of the most effective approaches. This technique alters the gel's microstructure, enhances its functionality, and improves its rheological properties (K. Liu et al., 2021).

Microalgae are also emerging as a promising source of both protein and carbohydrates for developing seafood substitutes (Drozdov & deClaville Christiansen, 2024).

Tetraselmis chui (TC) is a highly promising marine species characterized by a rapid growth and salt tolerance, which facilitates easier recycling of the culture media (Siddiqui et al., 2024). The nutritional potential of TC is noteworthy, as it has already received approval for food consumption in the European Union as a freeze-dried powder and boasts a protein content ranging from 30 to 50% dry weight. Recent studies have revealed that various marine microalgae, including TC, possess flavors reminiscent of seafood. This characteristic could prove valuable in the development of plant-based alternatives to seafood (Coleman et al., 2022; Moreira et al., 2022).

Yet, for the development of seafood analogs, it is also necessary to replicate the mimicking food composition, dietary benefits, and consistency of seafood and to reproduce their fibrous-gel configuration. 3D food printing is an advanced digital manufacturing technique that creates three-dimensional structures by layering liquid, gel, or powder food materials (Holland et al., 2018; Portanguen et al., 2019; Sun et al., 2015). The flexibility of 3D printing allows for the incorporation of alternative ingredients such as microalgae, enabling the production of flavorful, healthy, and customized food products (An et al., 2019; Godoi et al., 2016). Successful 3D printing requires a material that can be easily extruded while maintaining structural integrity to support subsequent layers. The quality of 3D-printed food is also influenced by the physicochemical properties of the ingredients and process parameters such as nozzle speed, extrusion rate, nozzle diameter, and layer and nozzle heights. The interplay between food formula attributes and operational conditions affects printing precision and end-product quality (Dankar et al., 2018; Pérez et al., 2019). Printed food items may require additional post-printing cooking processes like baking, boiling, or drying, which can lead to texture modifications and shape distortions due to varying heat penetration in the food matrix (Dankar et al., 2018; Sun et al., 2015).

The aim of this study was to assess the potential of TC and TC extract (E-TC) to be used as an ingredient in plant-based seafood alternatives and to compare their performance with pea protein (PP). The rheological and textural profile was analyzed as well as the color variation.

Materials and Methods

Raw Materials

PP (NUTRALYS® F85M) was provided by Roquette (Valencia, Spain), TC was supplied by Necton (Olhão, Portugal), and I-carrageenan was provided by Sosa Ingredients S.L. (Barcelona, Spain). The nutritional composition of the raw materials used is detailed in Table 1.

Microalgae Protein Extract Production

TC was diluted to reach a concentration of 10% (w/w) with distilled water (dH_2O). Thereafter, the microalgae were subjected to 4 cycles of freeze-thawing, as described in Moreira et al. (2025). Post-extraction, the resulting solution was centrifuged at 6000 g for 30 min, and the supernatants were carefully collected. The supernatants were then subjected to filtration using a pilot-scale filtration unit, Pellicon® 2 0.65 mm (Merck, Algés, Portugal), followed by ultrafiltration using a Pellicon® 2 Cassette with Ultracel® 5-kDa membrane. The filtration process was performed at room temperature. The extract was lyophilized for further use.

Protein Ink Preparation

A food ink (Table 2) was prepared using 2% I-carrageenan, 5% of protein source (PP, TC, and/or E-TC), and 93% dH_2O. First, 46.5% of dH_2O was heated to 80 °C using magnetic heating (VMS-C7, VWR International LLC., Leuven, Belgium), and the I-carrageenan gum was dissolved by stirring. The protein source (PP, TC, or E-TC) was mixed in another container at a concentration of 46.5% at room temperature for 15 min. The following combinations of protein sources were tested: PP at 5%, PP at 2.5% combined with TC at 2.5%, TC at 5%, PP at 5% with E-TC at 2.5%, and E-TC at 5%. After

Table 1 Nutritional composition of raw materials expressed in g/100 g

Composition	PP	TC	E-TC
Protein	62.85 ± 4.31%	32.33 ± 0.38%	24.00 ± 0.37%
Carbohydrates	20.65 ± 4.98%	9.99 ± 0.43%	58 ± 0.11%
Lipids	< 0.01%	22.76 ± 0.90%	< 0.01%
Ashes	5.17 ± 0.06%	32.95 ± 0.08%	40.06 ± 0.04%
Water	7.9 ± 0.40%	4.54 ± 0.03%	1.4 ± 0.22%

The proximal composition was characterized as described in Moreira et al., 2025 with lipids in PP and E-TC being calculated by different from 100% (Moreira et al., 2025). PP composition was provided by the supplier

PP, pea protein; *TC*, *Tetraselmis chui*; *E-TC*, extract from *Tetraselmis chui*

Table 2 Ink formulation for the development of the seafood analog

Ingredients	PP 5%	PP 2.5% + TC 2.5%	TC 5%	PP 2.5% + E-TC 2.5%	E-TC 5%
PP	5%	2.5%	-	2.5%	-
TC	-	2.5%	5%	-	-
E-TC	-	-	-	2.5%	5%
I-carrageenan	2%	2%	2%	2%	2%
dH_2O	93%	93%	93%	93%	93%

PP 5%, pea protein at 5% concentration; *PP 2.5% + TC 2.5%*, pea protein at 2.5% concentration and *Tetraselmis chui* at 2.5% concentration; *TC 5%*, *Tetraselmis chui* at 5% concentration; *PP 2.5% + E-TC 2.5%*, pea protein at 2.5% concentration and extract from *Tetraselmis chui* at 2.5% concentration; *E-TC 5%*, extract from *Tetraselmis chui* at 5% concentration

mixing the protein source into the I-carrageenan solution, the mixture's temperature was adjusted to 30 °C before printing.

3D Printing

This study employed a 3D food printer (BCN 3D+, BCN3D Technologies, Barcelona, Spain) equipped with an external water bath (PolyScience, IL, USA), to print the seafood analog. The 3D printing system consisted of an extrusion system (syringe plus pump) and an X–Y-Z positioning system using stepper motors. Printing was done at 40 °C, with a 0.06 mm^3/s extrusion rate and a nozzle diameter of 0.8 mm. A 4.5-cm-diameter and 1-cm-height prototype using Tinkercad (software from Autodesk, Inc., San Rafael, CA, USA) and the Ultimaker Cura software (version 5.7.1 developed by Ultimaker B.V, Brooklyn, NY, USA) was employed to set the printing parameters. The following parameters were used: a rectilinear infill of 100%, a layer height of 0.8 mm, and a speed of 10 mm/s.

Drying Process

The printed samples were frozen for 2 h at − 16 °C in a vertical freezer (CVF450/45, Ing. Climas, Barcelona, Spain). Subsequently, the samples were dried in a food dehydrator FD-600 (Back to Basics LTD, Lancashire, England) until reaching a humidity of 30 ± 5%.

Variation in Weight

The samples were weighed pre- and post-drying on a scale. The weight variation was determined according to Eq. 1 which shows the calculation of the percentage variation in weight.

$$\%\ \text{variation in weight} = \left[(\text{Pre drying weight} - \text{Post drying weigh})/\text{Pre drying weight}\right] \times 100 \quad (1)$$

Rheology Analysis

A HAAKE RheoStress 1 rheometer (Thermo, Waltham, MA, USA) with parallel plate 60 mm in diameter and 1.0 mm gap was used to perform oscillatory tests on the ink after printing. The linear viscoelastic region (LVR) was studied at 1 Hz from 0.1 to 10 Pa. The oscillatory test was performed in triplicate at a constant shear stress of 1 Pa and a frequency range of 0.1 to 10 Hz at 40 °C. Storage modulus (G′), loss modulus (G″), and complex viscosity |η*| were obtained via this analysis.

Extrusion Test

The printing conditions (velocity, temperature, syringe, and nozzle diameter) were replicated in the extrusion test. This extrusion test was performed using a TA.XT.plus texturometer (Stable Micro Systems, Godalming, Surrey, UK) and Texture Exponent 32 software (Stable Micro Systems, Godalming, Surrey, UK). The printer plunger, syringe with sample, and nozzle were placed on the texturometer, and a cylindrical press attachment was used to stabilize the syringe. The test conditions were 0.07-mm/s downstroke speed and 10-mm distance travelled (Barrios-Rodríguez et al., 2023). From the resulting curves, Extrusion force maximum (N) and extrusion area (N.s) parameters were obtained. The tests were performed in triplicate.

Texture Analysis

The texture profile analysis (TPA) of the seafood analogs after 3D printing was performed using the same TA.XT.plus texturometer used for extrusion tests. The TPA was conducted using a 4-cm-diameter cylindrical aluminum probe and a 50-kg load cell. The analysis was performed with double compression at a speed of 1 mm/s with a 5-s rest period between cycles and a 30% deformation of the original length.

The parameters of hardness, adhesiveness, cohesiveness, and springiness were extracted using the Texture Exponent 32 program. All samples were tested in triplicate.

Color Analysis

The color of the samples pre- and post-drying was determined by the CIEL*a*b* color space method. Color coordinates were obtained using a Konica Minolta CM-700d

colorimeter (Konica Minolta CM-700d/600d series, Tokyo, Japan) with standard illuminant D65 and a visual angle of 10°. Results were obtained in terms of L* (brightness: L* = 0 (black), L* = 100 (white)), a* (− a* = green, + a* = red), and b* (− b* = blue, + b* = yellow), according to the CIEL*a*b* system (Barrios-Rodríguez et al., 2023). From color coordinates, Chroma (C^*_{ab}, saturation) and hue angle (h^o_{ab}) were calculated. The total color difference (Δ E) between pre- and post-drying samples was determined using L*a*b* values according to Eq. 2. The measurements were conducted under constant lighting conditions, at room temperature °C.

$$\Delta E^* = \left[\left(\Delta L^*\right)^2 + (\Delta a^*)^2 + \left(\Delta b^*\right)^2\right]^{1/2} \quad (2)$$

Image Analysis

Images were taken of the top and front of each seafood analog printed. These images were analyzed using ImageJ software (ImageJ, NIH, Washington, DC, USA) to evaluate the dimensions and area of the figures. The base area was measured in the top view images, and the height was measured in the front view images, as illustrated in Table 1.

Data Processing, Fitting, and Analyses

Statistical analysis was conducted to determine significant differences based on the analysis of variance (ANOVA) using GraphPad Prism version 9.5.1 (GraphPad, CA, USA). For each table row, different superscript letters represent significant differences ($p < 0.05$). All values are reported as averages with standard deviation.

Results and Discussion

Protein Ink Evaluation

A comprehensive understanding of the entire 3D printing process is crucial for ensuring the quality and precision of the final product, as material characteristics may vary throughout. The extrusion test quantifies the force necessary for the piston to push the material through the printing nozzle. Compression curves offer vital insights into the maximum force required to print each sample and the specific needs of the extruder (Molina-Montero et al., 2023a). Table 3 displays the findings, including the extrusion maximum force (EF_M) and extrusion area (E_A) values for each sample. This evaluation plays a key role in fine-tuning 3D food printing parameters to guarantee optimal printability but also to compare formulation viscosity (Barrios-Rodríguez et al., 2023).

The E_A values obtained from the tested samples ranged from 575 to 4148 N.s. Inconsistent flow was observed in the initial measurements, particularly in the E-TC samples. In comparison to the PP 5%, the TC samples exhibited higher gradient values, with significant differences ($p < 0.05$), and the E-TC 5% sample was identified as the most challenging to print. The greater the E_A, the more effort is required during the extrusion process (MolIna-Montero et al., 2023b). Inks containing TC demand more effort to print than other formulations ($p < 0.05$).

In Fig. 1, it is possible to observe the force–time curves obtained during the extrusion test of the five inks. These curves demonstrate the various stages that occur as the gel is extruded. Initially, as the piston applies pressure to the sample, the force rises sharply until it reaches a peak, signaling the start of extrusion through the nozzle. Once the maximum force is attained, a plateau is observed, representing the average force required to sustain the extrusion process (Ares et al., 2006).

The slope of the curve is indicative of the gel's flow capacity, with a steeper slope suggesting higher extrusion force. In this experiment, TC 5% exhibited the steepest slope, indicating higher viscosity, followed by PP 5% and PP 2.5% + E-TC 2.5%. Both the slope and F_M are associated with the gel's stiffness and firmness (García-Segovia et al., 2020). Macroscopically, it was observed that E-TC 5% exhibited phase separation (see Table 4), which resulted in challenges during printing. These findings are corroborated by the extrusion test, where E-TC 5% demonstrated a highly irregular extrusion curve. The likely cause of the observed phenomenon is the sample's composition,

Table 3 Mean values and standard deviations of extrusion test

	PP 5%	PP 2.5% + TC 2.5%	TC 5%	PP 2.5% + E-TC 2.5%	E-TC 5%
EF_M (N)	38.3 ± 8.0	45.4 ± 9.9	63.0 ± 8.6	9.93 ± 0.36	52.8 ± 1.9
E_A (N.s)	2599 ± 263^a	3085 ± 733^{a,b}	4148 ± 584^b	575 ± 131^c	2398 ± 540^a

Mean values and standard deviations of EFM (extrusion force maximum) and EA (extrusion area) of inks during 3D printing. The values are expressed as means (SD) for five replicate experiments. Mean values with different letters within a same row are significantly different by ANOVA test at ($p < 0.05$)

PP 5%, pea protein at 5% concentration; *PP 2.5% + TC 2.5%*, pea protein at 2.5% concentration and *Tetraselmis chui* at 2.5% concentration; *TC 5%*, *Tetraselmis chui* at 5% concentration; *PP 2.5% + E-TC 2.5%*, pea protein at 2.5% concentration and extract from *Tetraselmis chui* at 2.5% concentration; *E-TC 5%*, extract from *Tetraselmis chui* at 5% concentration

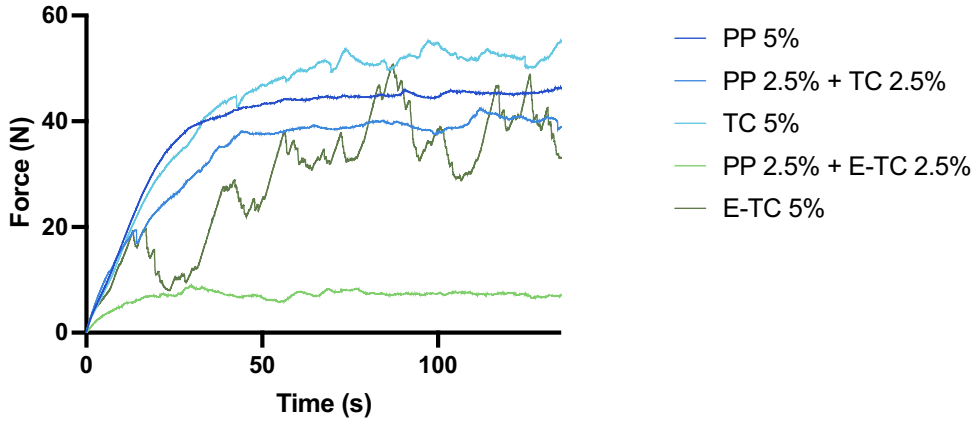


Fig. 1 Example of force vs. time curves during forward extrusion measurement for the five inks. Legend: PP 5%, pea protein at 5% concentration; PP 2.5% + TC 2.5%, pea protein at 2.5% concentration and *Tetraselmis chui* at 2.5% concentration; TC 5%, *Tetraselmis chui* at 5% concentration; PP 2.5% + E-TC 2.5%, pea protein at 2.5% concentration and extract from *Tetraselmis chui* at 2.5% concentration; E-TC 5%, extract from *Tetraselmis chui* at 5% concentration

characterized by increased carbohydrate and ash content. This composition may facilitate interactions within the matrix, leading to ink heterogeneity. Consequently, it is plausible that the particles in the sample are forming aggregates, which intermittently obstruct the needle and require additional force to maintain a consistent flow. The incorporation of both TC and E-TC content significantly affected the extrusion characteristics of the samples. While the addition of TC increased the ink's apparent viscosity, the inclusion of E-TC resulted in reduced viscosity (see Fig. 2). However, this latter observation is not evident in the results, possibly due to the ink's heterogeneity.

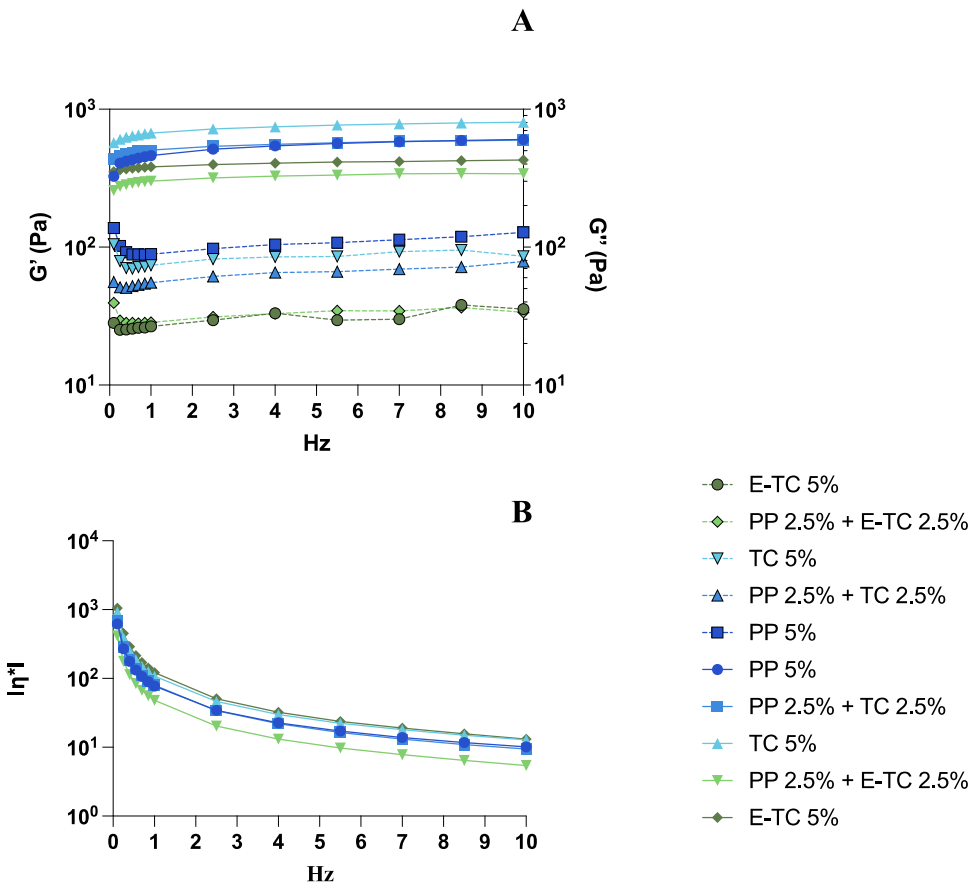


Fig. 2 Rheological properties of the inks. **A** Storage modulus G′, and loss modulus G″; **B** |η*|. In Fig. 2 A, upper lines represent G′ modulus, and bottom lines represent G″ modulus. Legend: PP 5%, pea protein at 5% concentration; PP 2.5% + TC 2.5%, pea protein at 2.5% concentration and *Tetraselmis chui* at 2.5% concentration; TC 5%, *Tetraselmis chui* at 5% concentration; PP 2.5% + E-TC 2.5%, pea protein at 2.5% concentration and extract from *Tetraselmis chui* at 2.5% concentration; E-TC 5%, extract from *Tetraselmis chui* at 5% concentration

Understanding the material's rheological and mechanical properties is crucial for achieving proper extrudability and structural stability (Z. Liu et al., 2018). A commonly employed technique for understanding rheological behavior after printing is small amplitude oscillatory rheological testing. This method involves applying stress or frequency that varies harmonically over time to the material (Norton et al., 2011). Typically, analysis is conducted descriptively based on G′, G″, and [η*] curves. When comparing different samples, researchers often examine values at specific frequencies (0.1 Hz and 10 Hz) (Cai et al., 2022; Hussain et al., 2021) providing quick insights into the rheological behavior of printing inks.

For a successful 3D food printing, the printing material must exhibit non-Newtonian viscoelastic rheological properties, specifically pseudoplastic. Pseudoplastic behavior is characterized by a decrease in viscosity as the shear rate increases (Barrulas & Corvo, 2023). This allows for sufficient viscosity to pass through the nozzle during extrusion, while also maintaining enough viscosity to fuse with previously deposited layers (Molina-Montero et al., 2023a). The elastic behavior of solids, represented by the G′, indicates the material's resistance to mechanical deformation. Conversely, the G″ represents the material's viscous response (Molina-Montero et al., 2023a). A predominance of the elastic modulus (G′ > G″) imparts solid-like properties to the material, indicating a greater ability to retain its structure after the printing process. The loss tangent (tan $\delta = G''/G'$) is a key parameter for evaluating this balance: when tan $\delta < 1$, elastic behavior predominates, which is favorable for maintaining the printed structure; when tan $\delta > 1$, viscous behavior dominates, which could compromise the structural stability (Tejada-Ortigoza & Cuan-Urquizo, 2022).

The viscoelastic parameters obtained from the oscillatory test conducted on the ink after 3D printing at < 30 °C showed the dynamic mechanical spectra of the ink samples as functions of frequency (Hz) in Fig. 2. Generally, the samples follow the same tendency as shown in the extrusion curves (Fig. 1). The samples containing E-TC exhibited the lowest G′ and G″ values. Conversely, TC 5% demonstrated the highest G′ behavior, followed by PP 5% and PP 2.5% + TC 2.5%, which displayed similar G′ curves. Additionally, the dynamic loss tangent (tan $\delta = G''/G'$) was below 1 for all inks, confirming the generic predominance of elastic behavior (Letras et al., 2022). Furthermore, it was noted that the G′ and G″ values of all samples demonstrated a largely frequency-independent response across the entire measurement range; this aligns with a tan $\delta < 1$ indicative of gel-like behavior. Generally, the magnitude of G′ is representative of hydrogel stiffness, while tan δ reflects elastic properties, with low tan δ values characteristic of ideal elastomers (Yan & Pochan, 2010). These mixtures exhibited elastic-like characteristics, with G′ exceeding G″ throughout the full range of angular frequencies. The tan δ values did not show significant variation among the five food samples (see Supplementary material Table 7) (Wang et al., 2023).

Compared with the PP 5%, the G′ of TC samples was continuously increased with the increase of the addition of *T. chui*, indicating that the addition of microalgae increased the number of entanglement points between the molecular chains in the gel system, enhancing the network structure, as also observed by Wang et al. (2023) with *Arthrospira platensis* suspension. This increase may be attributed to the ability of polysaccharides and fibers in microalgae to attract and bind water molecules, enhancing gel firmness (Letras et al., 2022). Research indicates that PP/starch systems exhibited more robust gels when microalgae are present (Batista et al., 2011). The addition of microalgal biomass may influence gel properties by altering pH and salt content, which affects PP electrostatic interactions during aggregation. These effects are likely more pronounced in microalgae biomass with higher ionic content and pH. Additionally, the overall macronutrient composition can impact the system (Batista et al., 2008). For instance, the carbohydrate, protein, and lipid profiles differ considerably between PP, TC, and E-TC. While PP 5% is composed of 62.85 ± 4.31% protein (w/w), TC and E-TC only have in their composition 32.33 ± 0.38% and 24.00 ± 0.37%, respectively. Yet, the internal components of microalgae are unlikely to be readily accessible for this type of interaction. Therefore, it is more probable that in the TC samples, these interactions occur with the constituents of the surface or the most superficial layer (Moreira et al., 2025). Conversely, the extrusion process in three-dimensional contexts may have induced some degree of permeabilization in the algal structure. A study performed by Drozdov and deClaville Christiansen (2024) observed that polysaccharides enhanced the functionality of protein-based gels by altering their microstructure and improving their rheological properties (Drozdov & deClaville Christiansen, 2024). But also, the presence of lipids could lead to alteration in the system (Houzé et al., 2005; Lucey et al., 1998; F. Vélez-Ruiz et al., 2005). Previous studies have shown that the changes in rheological properties of fat-containing gels are typically attributed to fat droplets functioning as active filler particles within the protein matrix. This could explain why TC G′ values are notably higher than those of E-TC ($p < 0.05$).

As shown in Fig. 2B, all samples presented a decrease in η* with increasing frequency, being a pseudoplastic fluid. This behavior of the samples is appropriate for 3D printing by extrusion, as the material will be able to flow easily through the nozzle due to the shear thinning that occurs

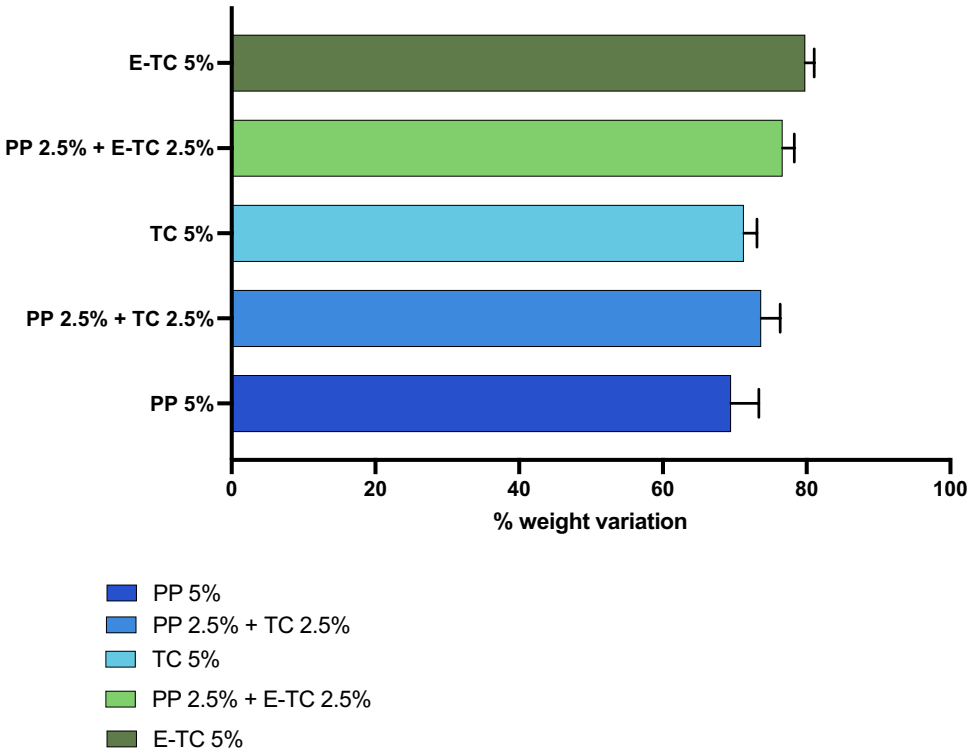
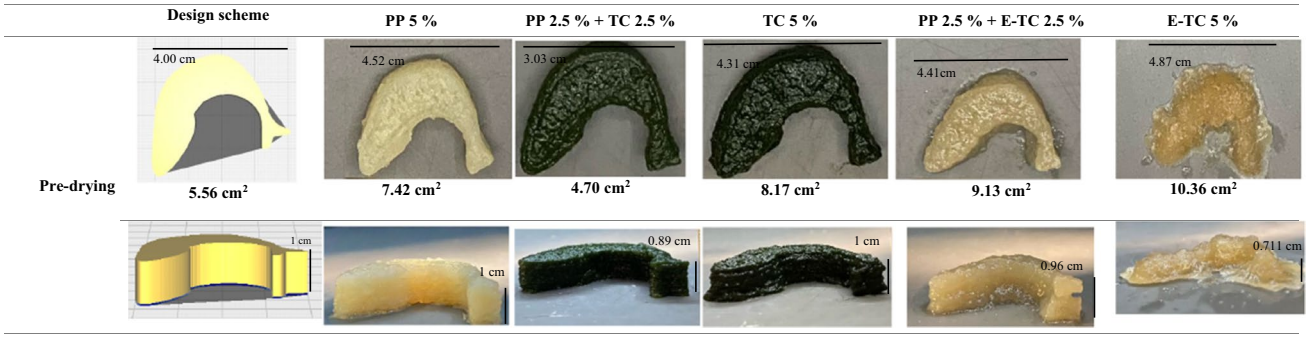


Fig. 3 Variation in weight (w/w %) between pre-and post-drying in the five testes samples. Legend: PP 5%, pea protein at 5% concentration; PP 2.5% + TC 2.5%, pea protein at 2.5% concentration and *Tetraselmis chui* at 2.5% concentration; TC 5%, *Tetraselmis chui* at 5% concentration; PP 2.5% + E-TC 2.5%, pea protein at 2.5% concentration and extract from *Tetraselmis chui* at 2.5% concentration; E-TC 5%, extract from *Tetraselmis chui* at 5% concentration

Table 4 3D-printed samples front and bird's-eye view after 3D printing process



PP 5%, pea protein at 5% concentration; *PP 2.5% + TC 2.5%*, pea protein at 2.5% concentration and *Tetraselmis chui* at 2.5% concentration; *TC 5%*, *Tetraselmis chui* at 5% concentration; *PP 2.5% + E-TC 2.5%*, pea protein at 2.5% concentration and extract from *Tetraselmis chui* at 2.5% concentration; *E-TC 5%*, extract from *Tetraselmis chui* at 5% concentration

when the applied stress exceeds the elastic limit and higher shape retention after 3D printing (Ares et al., 2006). In addition, viscosity is higher in TC 5% and lower in E-TC 5%. This can also be related to the quantity of carbohydrates, protein, and lipids present in the inks. PP 2.5% + E-TC 2.5% showed to have the lowest viscosity, which validates the data presented in the extrusion test (see Fig. 2).

Uribe-Wandurraga et al. (2020) observed that the increased microalgae (*Chlorella vulgaris* and *Arthospira platensis*) content resulted in higher G′ than G″ in batters, suggesting a solid-elastic-like behavior. A comparable observation was noted for also *Arthrospira platensis* and *Chlorella vulgaris* addition at 1.5% in breadstick doughs (Uribe-Wandurraga et al., 2019). In E-TC samples, no significant difference in G′ was observed when increasing from 2.5 to 5%. However, a change in viscoelastic behavior was noted when adding TC or E-TC compared to PP 5%.

Previous research indicates that microalgae extracts tend to denature rapidly and form gels at higher protein concentrations (10%), exhibiting elastic behavior (Garcia et al., 2018). Martin et al. (2014) proposed that during this phase, hydrophobic interactions and hydrogen bonds primarily contribute to the development of a stronger gel network. The potential absence of hydrophobic interactions in E-TC

is likely associated with decreased protein content, explaining this behavior.

Drying is employed to extract moisture from printed food products, thereby extending their longevity and enhancing their textural qualities. Additionally, dehydrated foods offer the benefits of being compact and easily transportable, making them exceptionally versatile for numerous applications (Waseem et al., 2024).

Figure 3 illustrates the weight changes in the printed food samples pre- and post-drying. No significant variations were observed among the samples, indicating that the drying process was carried out uniformly.

The pre-drying process of food samples revealed interesting results regarding the dimensional changes and structural integrity of different formulations (Table 4). PP 2.5% + TC 2.5% samples showed the closest resemblance to the original design, although the ink elastic-like behavior resulted in a retraction of the printed product, possibly due to the bound with polysaccharides which is reflected in lower area, width, and length. In contrast, E-TC 5% samples exhibited a structure that deviated significantly from the intended design after printing, with the E-TC 5% sample displaying a distinct gummy-like texture after drying, setting it apart from the other tested inks. This discrepancy may be attributed to the reduced protein content in the formulation, which could have affected its ability to form a stable hydrogel structure comparable to other formulations, as suggested by rheological and extrusion data.

The incorporation of PP and TC in the ink formulations resulted in varying macroscopic characteristics and textures. The PP 2.5% + TC 2.5% and PP 5% samples exhibited properties most like the original design. However, the presence of TC in the samples imparted a very dark green color, which could potentially be unappealing to consumers in food products. The presence of E-TC did not have this strong coloring effect. This highlights the importance of considering not only the functional properties but also the visual aspects of food ingredients in product development.

Evaluation of the Dry-Printed Products

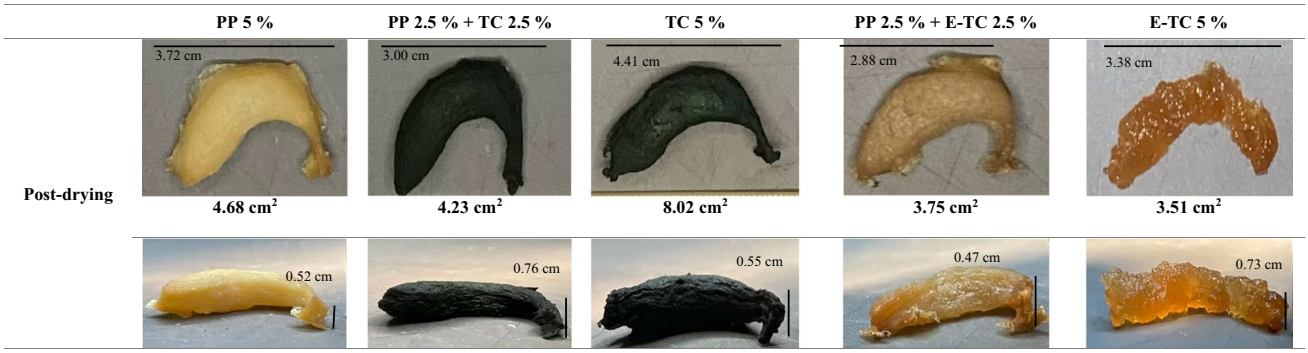
To evaluate the 3D printer's precision and the ink's ability to retain the desired form and structure, measurements of area, width, and length were taken also after the drying process (see Table 5). Macroscopic examination of the samples reveals that the incorporation of microalgae biomass noticeably altered the visual appearance of the product.

After drying, all products showed a reduction in area being more visible in the products with E-TC. The E-TC 5% sample displayed a distinct gummy-like texture, setting it apart from the other tested inks. These observations underscore the complex interplay between ingredient composition, concentration, and the resulting physical properties of the ink formulations, emphasizing the need for careful optimization to achieve the desired characteristics for specific applications.

Regarding dimensional measurements (width, length, and area) in comparison to PP 5%, only PP 2.5% + TC 2.5% exhibited a smaller area in the pre-drying samples, as also observed in pre-dried samples. The increase in TC and E-TC resulted in greater surface coverage, likely due to insufficient structure or bonding with water (more evident in E-TC 5%) (Batista et al., 2019). The sample length was shorter than PP 5%, although these samples displayed the greatest width. For post-drying samples, TC samples demonstrated the smallest reduction in area compared to pre-drying samples, while E-TC showed the largest. All samples decreased in width and length dimensions relative to pre-drying samples, with E-TC samples exhibiting a more pronounced lack of structure, further supported by rheometer and texturometer.

The shrinkage of dried samples in terms of area and length (%) is presented in Fig. 4. It was noted that samples with higher TC concentrations in their composition

Table 5 3D-printed samples front and bird's-eye view after drying process



PP 5%, pea protein at 5% concentration; *PP 2.5% + TC 2.5%*, pea protein at 2.5% concentration and *Tetraselmis chui* at 2.5% concentration; *TC 5%*, *Tetraselmis chui* at 5% concentration; *PP 2.5% + E-TC 2.5%*, pea protein at 2.5% concentration and extract from *Tetraselmis chui* at 2.5% concentration; *E-TC 5%*, extract from *Tetraselmis chui* at 5% concentration

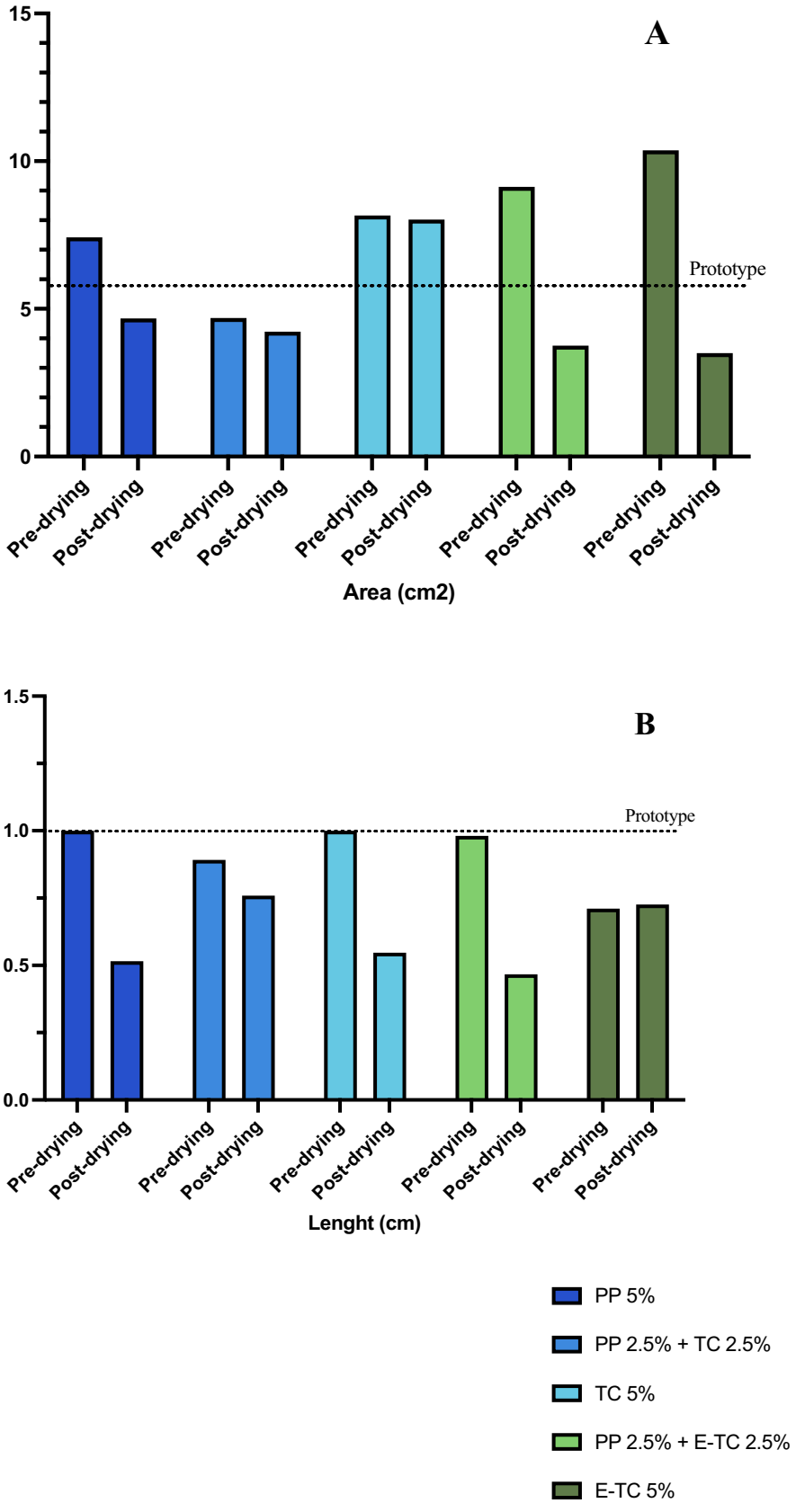


Fig. 4 Variation in area (**A**), and length (**B**) in between pre- and post-drying samples. Legend: PP 5%, pea protein at 5% concentration; PP 2.5% + TC 2.5%, pea protein at 2.5% concentration and *Tetraselmis chui* at 2.5% concentration; TC 5%, *Tetraselmis chui* at 5% concentration; PP 2.5% + E-TC 2.5%, pea protein at 2.5% concentration and extract from *Tetraselmis chui* at 2.5% concentration; E-TC 5%, extract from *Tetraselmis chui* at 5% concentration

exhibited less shrinkage. Conversely, E-TC demonstrated the greatest degree of shrinkage.

This effect can be explained by the increased protein-polysaccharide interaction, which could hinder water evaporation, limit inward contraction, and thus reduce shrinkage (MolIna-Montero et al., 2023b). Also, the formation of polysaccharide-protein complexes may result in robust connections between protein and polysaccharide molecules, as well as less intense physical interactions (such as electrostatic, hydrophobic, and van der Waals forces). This could lead to an overall improvement in the mechanical characteristics of the composite gels, resulting in a smaller reduction in area after the drying process (Drozdov & deClaville Christiansen, 2024) (Fig. 4).

When comparing initial areas to the design, only PP 5% and both samples with TC maintained a similar area. This suggests that E-TC are less effective in preserving the initial shape, resulting in a larger initial area and, consequently, more significant shrinkage.

While TC formulations provided good structural properties to the final product, the intense green color posed a challenge in achieving the desired shrimp-like appearance. Understanding these changes during the drying process can provide valuable insights for refining the formulation and processing parameters to achieve the desired characteristics in the final food product (see Table 5).

Textural Characterization of Printed Products

Food texture plays a crucial role in determining sensory attributes and structural integrity of food products. This study evaluated key textural parameters including hardness, cohesiveness, adhesiveness, and springiness (Table 6) to gain insights into solid properties that influence mouthfeel and practical applications (In et al., 2021). The findings revealed that the PP 5% formulation exhibited the highest hardness (2.042 ± 0.427 N), while E-TC 5% showed the lowest (0.362 ± 0.017 N). This aligns with the principle that elevated Tan δ values contribute to more compact structures with enhanced dimensional stability post-printing, present in Table 8 (In et al., 2021). As observed by other authors, the hardness of the products decreased while the concentration of microalgae increased (Batista et al., 2019; García-Segovia et al., 2017; Hernández-López et al., 2021, 2023; Palanisamy et al., 2019). Yet, De Gol et al., 2023 observed that the addition of *Chlorella vulgaris* in the PP formulation did not significantly affect hardness or anisotropy index observed in the extrudates (De Gol et al., 2023); this is probably due to the much higher dry matter content of the extrudates, while in the previous study, the moisture of the seafood analogs was kept the same between samples. A study performed by Caporgno et al. (2020) evaluated the potential of adding microalgae into the development of meat analogs. The results showed the incorporation of microalgae reduced the formation of a fibrous structure, leading to a reduction in cutting strength and hardness (Caporgno et al., 2020).

It was also observed that the incorporation of TC in the samples demonstrated lower adhesiveness values but higher cohesiveness, suggesting stronger molecule–molecule interactions potentially facilitated by carbohydrate binding forces (Caporgno et al., 2020). These results are in line with the data provided by the rheometer regarding the G′ modulus of TC when compared with PP. Further analysis of textural properties revealed interesting trends in springiness. Springiness, which measures a product′s ability to recover its original form after initial compression, showed significant variation only in the E-TC 5% sample, indicating its fragile nature.

Based on the printing settings employed and considering the intended application of the final product, it can be concluded that the optimal extrusion zone ranges from 38 to 65 N. The rheological and textural analyses revealed that TC, particularly at higher concentrations, provided better structural integrity and gel stability compared to PP. Generally, TPA showed that TC and E-TC affected the hardness and cohesiveness of the printed products. TC samples demonstrated higher cohesiveness, indicating

Table 6 TPA test parameters

	PP 5%	PP 2.5% + TC 2.5%	TC 5%	PP 2.5% + E-TC 2.5%	E-TC 5%
Hardness (N)	2.042 ± 0.427^{a}	1.351 ± 0.265^{b}	$1.648 \pm 0.438^{a,b}$	$1.541 \pm 0.383^{b,c}$	0.362 ± 0.017^{d}
Adhesiveness (N.s)	1.793 ± 0.091	0.000 ± 0.001^{a}	-0.015 ± 0.016^{a}	1.789 ± 0.157	1.498 ± 0.126
Cohesiveness (cm^2)	-0.002 ± 0.002	0.797 ± 0.032^{a}	0.847 ± 0.023^{a}	-0.078 ± 0.078	-0.087 ± 0.096
Springiness (cm)	0.673 ± 0.106	0.866 ± 0.132	0.929 ± 0.085	0.616 ± 0.154	0.174 ± 0.011^{a}

The values are expressed as means and standard deviations for five replicate experiments. Mean values with different letters within the same row are significantly different by ANOVA test at ($p < 0.05$)

PP 5%, pea protein at 5% concentration; *PP 2.5% + TC 2.5%*, pea protein at 2.5% concentration and *Tetraselmis chui* at 2.5% concentration; *TC 5%*, *Tetraselmis chui* at 5% concentration; *PP 2.5% + E-TC 2.5%*, pea protein at 2.5% concentration and extract from *Tetraselmis chui* at 2.5% concentration; *E-TC 5%*, extract from *Tetraselmis chui* at 5% concentration

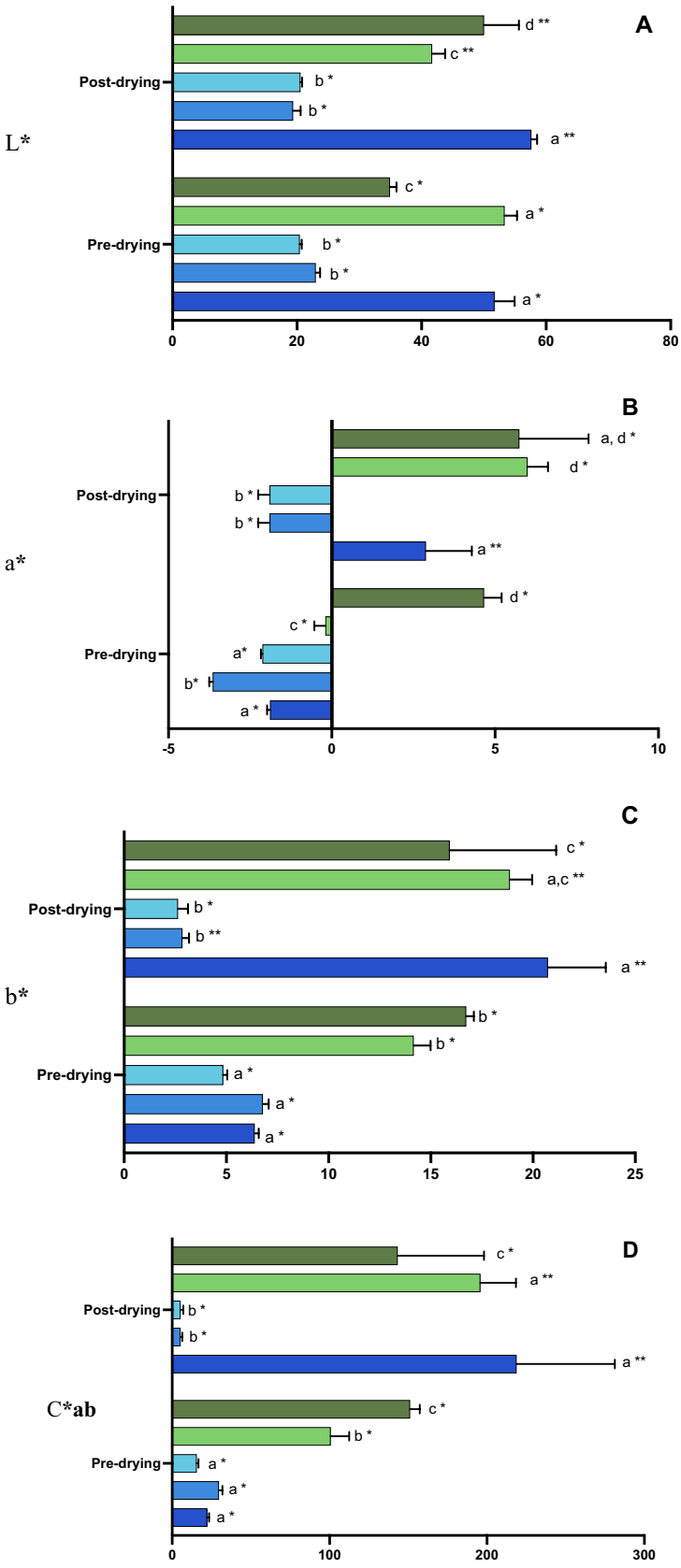
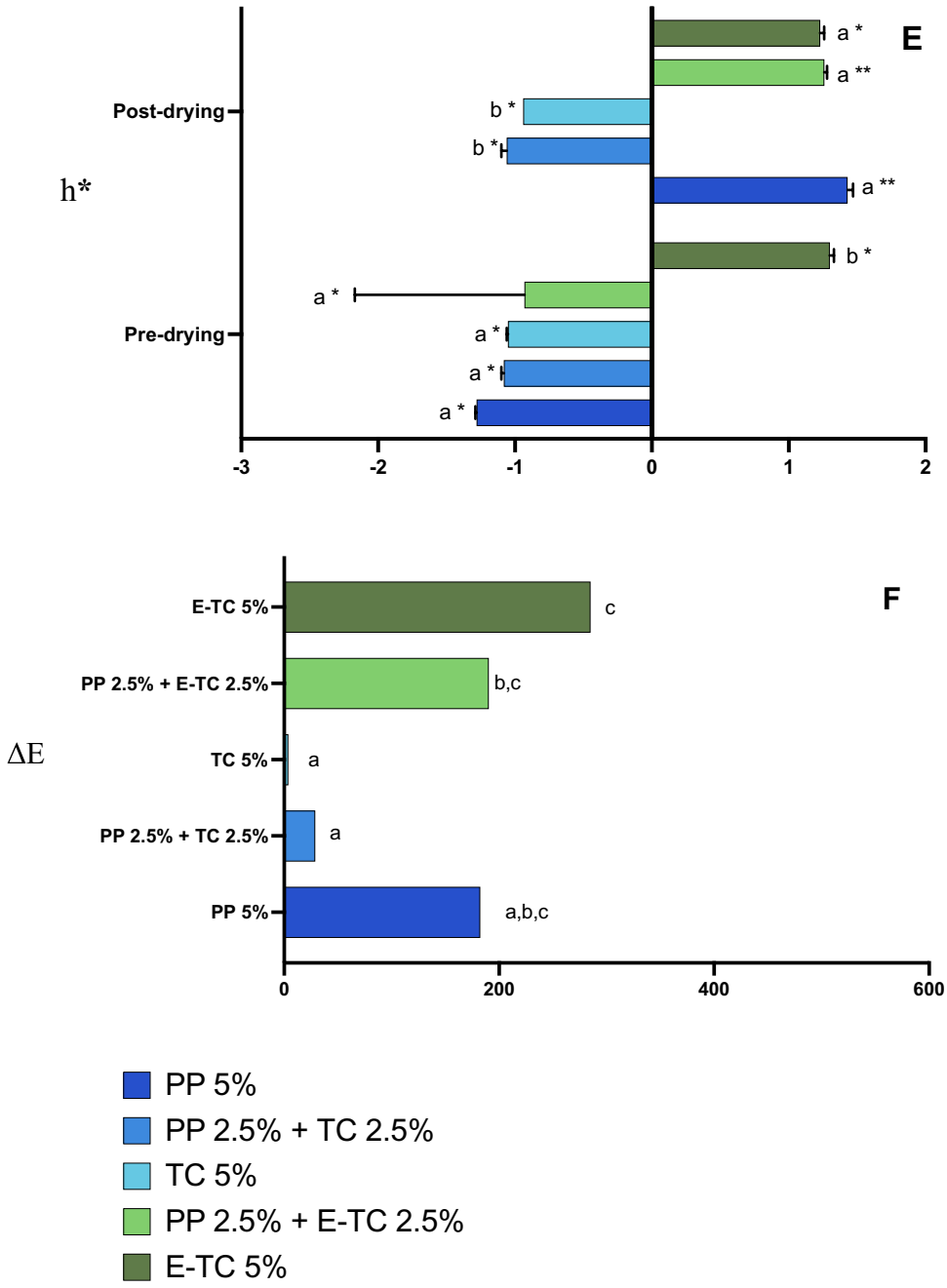


Fig. 5 Color parameters L* (**A**), a* (**B**), b* (**C**), h°ab (**D**), C*ab (**E**), and Δ*E* of printed samples pre- and post-drying (**F**). Different letter (a, b, c) within type of process (pre-drying, and post-drying) indicates statistical differences between groups established by ANOVA ($p < 0.05$), different symbol (*, **) within the same sample indicates statistical difference during drying process established by ANOVA ($p < 0.05$). Legend: PP 5%, pea protein at 5% concentration; PP 2.5% + TC 2.5%, pea protein at 2.5% concentration and *Tetraselmis chui* at 2.5% concentration; TC 5%, *Tetraselmis chui* at 5% concentration; PP 2.5% + E-TC 2.5%, pea protein at 2.5% concentration and extract from *Tetraselmis chui* at 2.5% concentration; E-TC 5%, extract from *Tetraselmis chui* at 5% concentration

Fig. 5 (continued)



stronger molecular interactions and a more stable gel network. The lower hardness of E-TC samples suggests a softer texture, which could be desirable for certain seafood analogues.

Color Analysis in the Post-drying Products

Food product acceptability is significantly influenced by color, which is determined by the ink's physicochemical properties (such as water content, pH, reducing sugars, and amino acid content) and the baking conditions (specifically the drying process) (Batista et al., 2013; García-Segovia et al., 2017). Figure 5 illustrates the color changes in printed samples before and after drying, expressed as lightness (L*), which ranges from 0 (black) to 100 (white), greenness (−)/redness (+) identify as a*, blueness (−)/yellowness (+) identify as b*, hue (h°ab), chroma (C*ab), and total color difference (Δ E).

Pre-drying L* values showed significant differences ($p < 0.05$) between PP 5%, TC samples, and E-TC 5%. This trend persisted in post-drying samples, although only the samples with E-TC 2.5% exhibited significant L* changes from pre- to post-drying. Overall, L* decreased notably with microalgae addition, although PP2.5% + TC 2.5% showed no

Table 7 Detailed summary of available studies on microalgae-based 3D food products

Microalgae biomass	Quantity	Type of product	Technology employed	Main results	References
Arthrospira platensis *Chlorella vulgaris*	1–4%	snacks	3D printing	Snacks with 3% and 4% microalgae enrichment produced the most precise printed structures	Uribe-Wandurraga et al. (2020)
Chlorella vulgaris	2–30%	snacks	3D printing	Up to 12% microalgae incorporation in dough presented most accurate structures Increasing additions of microalga led to higher values of total color difference	Oliveira et al. (2022)
Arthrospira platensis	5–10%	Gluten-free cereals	3D printing	Best results obtained 5–10% microalgal biomass in terms of rheological and printing behavior 5% Spirulina presented better nutritional and sensory properties	Letras et al. (2022)
Azolla fillicuiloids	5–20%	Gluten free snacks	3D printing	The process of printing doughs proved to be efficient 5% microalgae, enhancing antioxidant properties	Hassan et al. (2025)

significant L* differences from TC 5%. PP 2.5% + E-TC 2.5% showed higher light in pre-drying samples than E-TC 5%, yet post-drying samples showed an inverse tendency, eventually corresponding to some algae pigment degradation (oxidation) with the drying process, making the sample less dark. Pre-drying a* values for PP 5%, PP 2.5% + TC 2.5%, TC 5%, and PP 2.5% + E-TC 2.5% were negative, corresponding to a more greenish samples, although the last one showed the higher negative value ($p < 0.05$). E-TC 5% samples had positive values without significant differences between pre- and post-drying. As expected, the TC maintained the negative values (corresponding to a greener sample), eventually also associated with some pigment degradation, turning the samples more reddish/brownish. This effect may be associated with a higher pigment degradation of chlorophyll and carotenoids because of the drying process or with a pigment saturation, contributing to color changes in microalgae-enriched snacks (Batista et al., 2019). This pattern aligns with observations by other researchers in cookies with *Arthrospira platensis* biomass addition (Vieira et al., 2020).

Regarding yellowness, pre-drying E-TC samples had the highest b* values ($p < 0.05$), while PP 5% and TC samples were similar. Post-drying, PP 5% showed a considerable b* increase, PP 2.5% + TC 2.5% decreased, and PP 2.5% + E-TC 2.5% increased significantly. For microalgae, the a* and b* values can be particularly useful in assessing chlorophyll and lipid content. Research has shown that these color coordinates can be modeled as linear correlation functions for microalgal chlorophyll and lipid contents, with a squared correlation coefficient (R^2) of 0.99 for both parameters (Su et al., 2008).

C*ab, which represents the saturation or intensity of a color, varied substantially between TC and E-TC samples both pre- and post-drying. PP 5% exhibited increased chroma post-drying. ΔE values between pre- and post-drying samples indicated the most significant color transitions in samples without TC, as observed macroscopically in Table 5. Nevertheless, the consumer may regard this change in color (to a more reddish/brownish color) as a characteristic behavior of a cooked shrimp analogue, which is not necessarily negative. The minimal changes in TC samples during drying may be attributed to the dominant green pigment in microalgae, which remains stable during drying. Literature suggests that $\Delta E > 3$ indicates a perceivable color difference for consumers (García-Segovia et al., 2017).

The drying process affected the dimensional stability of the printed products. TC samples exhibited less shrinkage compared to E-TC, indicating better retention of the original shape and size. This is crucial for maintaining the structural integrity and appearance of 3D-printed food products. The color analysis indicated that while TC imparted a green hue to the products, it maintained color stability during the drying process.

Formulations containing TC exhibit more elastic behavior, rendering them suitable for 3D printing. The absence of structural integrity in formulations with E-TC may be attributed to their lower protein content. Therefore, in the future, when developing formulations for similar products, it would be beneficial to use higher concentrations of E-TC and/or include biopolymers like agar or alginate that could offer structural reinforcement to the matrix.

A few studies have investigated the incorporation of microalgae into food products with the objective of enhancing their nutritional quality and rheological properties during 3D printing processes. Table 7 presents a comprehensive summary of these studies focusing on microalgae-based 3D food products. The results indicate that the inclusion of small quantities (up to 5%) of microalgae can improve both the rheological behavior and overall nutritional profile without adversely affecting sensory characteristics (Hassan et al., 2025; Letras et al., 2022; Uribe-Wandurraga et al., 2020). However, it is noteworthy that a change in color is frequently observed as a result of this incorporation (Oliveira et al., 2022).

Conclusion

This research explored the potential of utilizing TC and its E-TC in the creation of 3D-printed seafood analogues. The formulation of plant protein–polysaccharide hydrogels and emulsion gels as inks for 3D food printing presents significant challenges due to their rheological properties. TC samples have shown promise as an ingredient in food product development, particularly due to their superior stress tolerance in shear rate assessments. Nonetheless, a notable drawback is their pronounced dark green coloration. If the aim were to produce a dark-colored product instead of a seafood analogue, this characteristic could be beneficial in enhancing the nutritional profile of the food product with these microalgae. Future investigations should aim to refine the formulation and processing parameters to improve the sensory qualities and consumer acceptance of these novel food products. Furthermore, research should focus on methods to reduce the pigmentation of the microalgae while preserving its functional properties.

Supplementary Information The online version contains supplementary material available at https://doi.org/10.1007/s11947-025-03965-9.

Author Contributions CM: conceptualization, formal analysis, investigation, methodology, visualization, data processing, writing – original draft. CMM: investigation, methodology, visualization, data processing, writing – original draft. PF-S: conceptualization, methodology, validation, supervision, writing – review and editing, formal analysis. JAT: validation, writing – review & editing, supervision, resources, funding acquisition, formal analysis. CR: conceptualization, methodology, formal analysis, validation, supervision, resources, writing – review and editing. JM: conceptualization, methodology, validation, resources, supervision, formal analysis writing – review and editing.

Funding Open Access funding provided thanks to the CRUE-CSIC agreement with Springer Nature. This study was also supported by the Portuguese Foundation for Science and Technology (FCT) under the scope of the strategic funding of UIDB/04469/2020 unit and LA/P/0029/2020 (LABBELS – Associate Laboratory in Biotechnology, Bioengineering and Microelectromechanical Systems). Catarina Moreira is a recipient of PhD scholarships supported by FCT (Ref. 2021.05734.BD), and Carmen Molina-Montero holds a FPI PhD contract granted by the Universitat Politècnica de Valencia subprograma 1 (PAID 01 21). Pedro Ferreira-Santos received support from the Consellería de Educación, Ciencia, Universidades e Formación Profesional of Xunta de Galicia, and the University of Vigo through a postdoctoral contract (reference 0623–137919) under the agreement for the development of strategic actions at the Campus Auga—Ourense (2024–2027). Javier Martínez Monzó received financial support from the Generalitat Valenciana (AGROALNEXT/2022/001).

Data Availability The datasets obtained during the current study are available from the corresponding author upon reasonable request.

Declarations

Competing interests The authors declare no competing interests.

Open Access This article is licensed under a Creative Commons Attribution 4.0 International License, which permits use, sharing, adaptation, distribution and reproduction in any medium or format, as long as you give appropriate credit to the original author(s) and the source, provide a link to the Creative Commons licence, and indicate if changes were made. The images or other third party material in this article are included in the article's Creative Commons licence, unless indicated otherwise in a credit line to the material. If material is not included in the article's Creative Commons licence and your intended use is not permitted by statutory regulation or exceeds the permitted use, you will need to obtain permission directly from the copyright holder. To view a copy of this licence, visit http://creativecommons.org/licenses/by/4.0/.

References

An, Y., Guo, C., Zhang, M., & Zhong, Z. (2019). Investigation on characteristics of 3D printing using *Nostoc sphaeroides* biomass. *Journal of the Science of Food and Agriculture, 99*(2), 639–646. https://doi.org/10.1002/jsfa.9226

Ares, G., Giménez, A. N. A., & Gámbaro, A. (2006). Instrumental methods to characterize nonoral texture of dulce de leche. *Journal of Texture Studies, 37*(5), 553–567.

Barrios-Rodríguez, Y. F., Igual-Ramo, M., Martínez-Monzó, J., & García-Segovia, P. (2023). Effect of food 3d printing process on the rheological properties of rice protein printing inks. *Foods, 2023*, 15. https://doi.org/10.3390/Foods2023-15061

Barrulas, R. V., & Corvo, M. C. (2023). Rheology in product development: An insight into 3D printing of hydrogels and aerogels. *Gels, 9*(12), 986. https://doi.org/10.3390/gels9120986

Batista, A. P., Gouveia, L., Bandarra, N. M., Franco, J. M., & Raymundo, A. (2013). Comparison of microalgal biomass profiles as novel functional ingredient for food products. *Algal Research, 2*(2), 164–173. https://doi.org/10.1016/j.algal.2013.01.004

Batista, A. P., Gouveia, L., Nunes, M. C., Franco, J. M., & Raymundo, A. (2008). Microalgae biomass as a novel functional ingredient in mixed gel systems. In *Gums and Stabilisers for the Food Industry 14* (pp. 487–494). The Royal Society of Chemistry. https://doi.org/10.1039/9781847558312-00487

Batista, A. P., Niccolai, A., Bursic, I., Sousa, I., Raymundo, A., Rodolfi, L., Biondi, N., & Tredici, M. R. (2019). Microalgae as functional ingredients in savory food products: Application to wheat crackers. *Foods, 8*(12), 611. https://doi.org/10.3390/foods8120611

Batista, A. P., Nunes, M. C., Raymundo, A., Gouveia, L., Sousa, I., Cordobés, F., Guerrero, A., & Franco, J. M. (2011). Microalgae

biomass interaction in biopolymer gelled systems. *Food Hydrocolloids, 25*(4), 817–825. https://doi.org/10.1016/j.foodhyd.2010.09.018

Cai, Q., Zhong, Y., Xu, M., Huang, Q., & Lu, X. (2022). 3D printed high oil custard cream: Effects of whey protein isolate, hydroxypropylated starch and carrageenan on physicochemical properties and printing performance. *LWT, 156*, Article 113039. https://doi.org/10.1016/j.lwt.2021.113039

Caporgno, M. P., Böcker, L., Müssner, C., Stirnemann, E., Haberkorn, I., Adelmann, H., Handschin, S., Windhab, E. J., & Mathys, A. (2020). Extruded meat analogues based on yellow, heterotrophically cultivated Auxenochlorella protothecoides microalgae. *Innovative Food Science & Emerging Technologies, 59*, Article 102275. https://doi.org/10.1016/j.ifset.2019.102275

Coleman, B., Van Poucke, C., Dewitte, B., Ruttens, A., Moerdijk-Poortvliet, T., Latsos, C., De Reu, K., Blommaert, L., Duquenne, B., Timmermans, K., van Houcke, J., Muylaert, K., & Robbens, J. (2022). Potential of microalgae as flavoring agents for plant-based seafood alternatives. *Future Foods, 5*, Article 100139. https://doi.org/10.1016/j.fufo.2022.100139

Dankar, I., Haddarah, A., Omar, F. E. L., Sepulcre, F., & Pujolà, M. (2018). 3D printing technology: The new era for food customization and elaboration. *Trends in Food Science & Technology, 75*, 231–242. https://doi.org/10.1016/j.tifs.2018.03.018

De Gol, C., Snel, S., Rodriguez, Y., & Beyrer, M. (2023). Gelling capacity of cell-disrupted Chlorella vulgaris and its texture effect in extruded meat substitutes. *Food Structure, 37*, Article 100332. https://doi.org/10.1016/j.foostr.2023.100332

Drozdov, A. D., & deClaville Christiansen, J. (2024). Rheology of plant protein–polysaccharide gel inks for 3D food printing: Modeling and structure–property relations. *Journal of Food Engineering, 380*, Article 112150. https://doi.org/10.1016/j.jfoodeng.2024.112150

F. Vélez-Ruiz, J., González-Tomás, L., & Costell, E. (2005). Rheology of dairy custard model systems: Influence of milk-fat and hydrocolloid type. *European Food Research and Technology*, *221*(3–4), 342–347. https://doi.org/10.1007/s00217-005-1174-8

García-Segovia, P., García-Alcaraz, V., Balasch-Parisi, S., & Martínez-Monzó, J. (2020). 3D printing of gels based on xanthan/konjac gums. *Innovative Food Science & Emerging Technologies, 64*, Article 102343.

García-Segovia, P., Pagán-Moreno, M. J., Lara, I. F., & Martínez-Monzó, J. (2017). Effect of microalgae incorporation on physicochemical and textural properties in wheat bread formulation. *Food Science and Technology International, 23*(5), 437–447. https://doi.org/10.1177/1082013217700259

Garcia, E. S., van Leeuwen, J. J. A., Safi, C., Sijtsma, L., van den Broek, L. A. M., Eppink, M. H. M., Wijffels, R. H., & van den Berg, C. (2018). Techno-functional properties of crude extracts from the green microalga *Tetraselmis suecica*. *Journal of Agricultural and Food Chemistry, 66*(29), 7831–7838. https://doi.org/10.1021/acs.jafc.8b01884

Godoi, F. C., Prakash, S., & Bhandari, B. R. (2016). 3d printing technologies applied for food design: Status and prospects. *Journal of Food Engineering, 179*, 44–54. https://doi.org/10.1016/j.jfoodeng.2016.01.025

Good Food Institute. (2022). *The big idea. 2022 Year in Review*. OER Commons. Retrieved March 12, 2025, from https://gfi.org/wpcontent/uploads/2023/01/GFI22007_year-in-review-2022_spreads_WEB.pdf

Hadidi, M., Jafarzadeh, S., Forough, M., Garavand, F., Alizadeh, S., Salehabadi, A., Khaneghah, A. M., & Jafari, S. M. (2022). Plant protein-based food packaging films; recent advances in fabrication, characterization, and applications. *Trends in Food Science & Technology, 120*, 154–173.

Hassan, I., Rasheed, N., Gani, A., & Gani, A. (2025). Rice starch, millet flour supplemented with algal biomass for 3D food printing. *International Journal of Biological Macromolecules, 303*, Article 140604. https://doi.org/10.1016/j.ijbiomac.2025.140604

Hernández-López, I., Abadias, M., Prieto-Santiago, V., Chic-Blanco, Á., Ortiz-Solà, J., & Aguiló-Aguayo, I. (2023). Exploring the nutritional potential of microalgae in the formulation of bakery products. *Foods, 13*(1), 84. https://doi.org/10.3390/foods13010084

Hernández-López, I., Benavente Valdés, J. R., Castellari, M., Aguiló-Aguayo, I., Morillas-España, A., Sánchez-Zurano, A., Acién-Fernández, F. G., & Lafarga, T. (2021). Utilisation of the marine microalgae Nannochloropsis sp. and Tetraselmis sp. as innovative ingredients in the formulation of wheat tortillas. *Algal Research*, *58*, 102361. https://doi.org/10.1016/j.algal.2021.102361

Holland, S., Tuck, C., & Foster, T. (2018). Selective recrystallization of cellulose composite powders and microstructure creation through 3D binder jetting. *Carbohydrate Polymers, 200*, 229–238. https://doi.org/10.1016/j.carbpol.2018.07.064

Houzé, G., Cases, E., Colas, B., & Cayot, P. (2005). Viscoelastic properties of acid milk gel as affected by fat nature at low level. *International Dairy Journal, 15*(10), 1006–1016. https://doi.org/10.1016/j.idairyj.2004.09.007

Hussain, S., Arora, V. K., & Malakar, S. (2021). Formulation of protein-enriched 3D printable food matrix and evaluation of textural, rheological characteristics, and printing stability. *Journal of Food Processing and Preservation*, *45*(2). https://doi.org/10.1111/jfpp.15182

In, J., Jeong, H., Song, S., & Min, S. C. (2021). Determination of material requirements for 3D gel food printing using a fused deposition modeling 3D printer. *Foods, 10*(10), 2272. https://doi.org/10.3390/foods10102272

Kazir, M., & Livney, Y. D. (2021). Plant-based seafood analogs. *Molecules, 26*(6), 1559. https://doi.org/10.3390/molecules26061559

Letras, P., Oliveira, S., Varela, J., Nunes, M. C., & Raymundo, A. (2022). 3D printed gluten-free cereal snack with incorporation of Spirulina (Arthrospira platensis) and/or Chlorella vulgaris. *Algal Research, 68*, Article 102863. https://doi.org/10.1016/j.algal.2022.102863

Liu, K., Chen, Y.-Y., Zha, X.-Q., Li, Q.-M., Pan, L.-H., & Luo, J.-P. (2021). Research progress on polysaccharide/protein hydrogels: Preparation method, functional property and application as delivery systems for bioactive ingredients. *Food Research International, 147*, Article 110542. https://doi.org/10.1016/j.foodres.2021.110542

Liu, Z., Zhang, M., Bhandari, B., & Yang, C. (2018). Impact of rheological properties of mashed potatoes on 3D printing. *Journal of Food Engineering, 220*, 76–82. https://doi.org/10.1016/j.jfoodeng.2017.04.017

Lucey, J. A., Munro, P. A., & Singh, H. (1998). Rheological properties and microstructure of acid milk gels as affected by fat content and heat treatment. *Journal of Food Science, 63*(4), 660–664. https://doi.org/10.1111/j.1365-2621.1998.tb15807.x

Martin, A. H., Nieuwland, M., & de Jong, G. A. H. (2014). Characterization of heat-set gels from RuBisCO in comparison to those from other proteins. *Journal of Agricultural and Food Chemistry, 62*(44), 10783–10791. https://doi.org/10.1021/jf502905g

Molina-Montero, C., Matas, A., Igual, M., Martínez-Monzó, J., & García-Segovia, P. (2023a). Impact of apricot pulp concentration on cylindrical gel 3D printing. *Gels, 9*(3), 253. https://doi.org/10.3390/gels9030253

Molina-Montero, C., Vicente-Jurado, D., Igual, M., Martínez-Monzó, J., & García-Segovia, P. (2023b). Fiber enrichment of 3D printed apricot gel snacks with orange by-products. *Gels, 9*(7), 569. https://doi.org/10.3390/gels9070569

Moreira, C., Ferreira-Santos, P., Nunes, R., Carvalho, B., Pereira, H., Teixeira, J. A., & Rocha, C. M. R. (2025). Influence of different processing techniques on microalgal protein extraction. *Algal Research, 86*, Article 103958. https://doi.org/10.1016/j.algal.2025.103958

Moreira, C., Ferreira-Santos, P., Teixeira, J. A., & Rocha, C. M. R. (2022). Active aroma compounds assessment of processed and non-processed micro- and macroalgae by solid-phase microextraction and gas chromatography/mass spectrometry targeting seafood analogs. *Frontiers in Sustainable Food Systems*, *6*. https://doi.org/10.3389/fsufs.2022.1011020

Norton, I. T., Spyropoulos, F., & Cox, P. (Eds.). (2011). *Practical food rheology*. Wiley. https://doi.org/10.1002/9781444391060

Oliveira, S., Sousa, I., & Raymundo, A. (2022). Printability evaluation of Chlorella vulgaris snacks. *Algal Research, 68*, Article 102879. https://doi.org/10.1016/j.algal.2022.102879

Palanisamy, M., Töpfl, S., Berger, R. G., & Hertel, C. (2019). Physico-chemical and nutritional properties of meat analogues based on Spirulina/lupin protein mixtures. *European Food Research and Technology, 245*(9), 1889–1898. https://doi.org/10.1007/s00217-019-03298-w

Pérez, B., Nykvist, H., Brøgger, A. F., Larsen, M. B., & Falkeborg, M. F. (2019). Impact of macronutrients printability and 3D-printer parameters on 3D-food printing: A review. *Food Chemistry, 287*, 249–257. https://doi.org/10.1016/j.foodchem.2019.02.090

Portanguen, S., Tournayre, P., Sicard, J., Astruc, T., & Mirade, P.-S. (2019). Toward the design of functional foods and biobased products by 3D printing: A review. *Trends in Food Science & Technology, 86*, 188–198. https://doi.org/10.1016/j.tifs.2019.02.023

Ren, W., Xia, W., Gunes, D. Z., & Ahrné, L. (2024). Heat-induced gels from pea protein soluble colloidal aggregates: Effect of calcium addition or pH adjustment on gelation behavior and rheological properties. *Food Hydrocolloids, 147*, Article 109417. https://doi.org/10.1016/j.foodhyd.2023.109417

Siddiqui, S. A., Ucak, İ, Afreen, M., Sasidharan, A., Yunusa, B. M., Bhowmik, S., Pandiselvam, R., Ambartsumov, T. G., & Shah, M. A. (2024). Microalgae as a potential raw material for plant-based seafood alternatives: A comprehensive review. *Food Science & Nutrition, 12*(11), 8559–8593. https://doi.org/10.1002/fsn3.4313

Su, C., Fu, C., Chang, Y., Nair, G. R., Ye, J., Chu, I. -Ming, & Wu, W. (2008). Simultaneous estimation of chlorophyll a/ and lipid contents in microalgae by three-color analysis. *Biotechnology and Bioengineering*, *99*(4), 1034–1039. https://doi.org/10.1002/bit.21623

Sun, J., Zhou, W., Huang, D., Fuh, J. Y. H., & Hong, G. S. (2015). An overview of 3D printing technologies for food fabrication. *Food and Bioprocess Technology, 8*(8), 1605–1615. https://doi.org/10.1007/s11947-015-1528-6

Tejada-Ortigoza, V., & Cuan-Urquizo, E. (2022). Towards the development of 3D-Printed food: A rheological and mechanical approach. *Foods, 11*(9), 1191. https://doi.org/10.3390/foods11091191

United Nations, Department of Economic and Social Affairs, Population Division. (2019). *World population prospects 2019: Highlights* (ST/ESA/SER.A/423). United Nations.

Uribe-Wandurraga, Z. N., Igual, M., García-Segovia, P., & Martínez-Monzó, J. (2019). Effect of microalgae addition on mineral content, colour and mechanical properties of breadsticks. *Food & Function, 10*(8), 4685–4692. https://doi.org/10.1039/C9FO00286C

Uribe-Wandurraga, Z. N., Zhang, L., Noort, M. W. J., Schutyser, M. A. I., García-Segovia, P., & Martínez-Monzó, J. (2020). Printability and physicochemical properties of microalgae-enriched 3D-printed snacks. *Food and Bioprocess Technology, 13*(11), 2029–2042. https://doi.org/10.1007/s11947-020-02544-4

Vieira, M. V., Oliveira, S. M., Amado, I. R., Fasolin, L. H., Vicente, A. A., Pastrana, L. M., & Fuciños, P. (2020). 3D printed functional cookies fortified with Arthrospira platensis: Evaluation of its antioxidant potential and physical-chemical characterization. *Food Hydrocolloids, 107*, Article 105893. https://doi.org/10.1016/j.foodhyd.2020.105893

Wang, M., Yin, Z., Sun, W., Zhong, Q., Zhang, Y., & Zeng, M. (2023). Microalgae play a structuring role in food: Effect of spirulina platensis on the rheological, gelling characteristics, and mechanical properties of soy protein isolate hydrogel. *Food Hydrocolloids, 136*, Article 108244. https://doi.org/10.1016/j.foodhyd.2022.108244

Waseem, M., Tahir, A. U., & Majeed, Y. (2024). Printing the future of food: The physics perspective on 3D food printing. *Food Physics, 1*, Article 100003. https://doi.org/10.1016/j.foodp.2023.100003

Wen, Y., Chao, C., Che, Q. T., Kim, H. W., & Park, H. J. (2023). Development of plant-based meat analogs using 3D printing: Status and opportunities. *Trends in Food Science & Technology, 132*, 76–92.

Yan, C., & Pochan, D. J. (2010). Rheological properties of peptide-based hydrogels for biomedical and other applications. *Chemical Society Reviews, 39*(9), 3528. https://doi.org/10.1039/b919449p

Zhong, C., Feng, Y., & Xu, Y. (2023). Production of fish analogues from plant proteins: Potential strategies, challenges, and outlook. *Foods, 12*(3), 614.

Publisher's Note Springer Nature remains neutral with regard to jurisdictional claims in published maps and institutional affiliations.